Desalination and Water Treatment
www.deswater.com
doi: 10.1080/19443994.2014.888684

54 (2015) 1651–1662
May

Taylor & Francis
Taylor & Francis Group

On the importance of surface chemistry and composition of Bone char for the sorption of heavy metals from aqueous solution

Didilia I. Mendoza-Castillo[a], Adrián Bonilla-Petriciolet[a,*], Juan Jáuregui-Rincón[b]

[a]*Chemical Engineering Department, Instituto Tecnológico de Aguascalientes, Av. López Mateos 1801, Aguascalientes, México*
Tel. +52 4 49910 5002x127; email: petriciolet@hotmail.com
[b]*Biochemical Engineering Department, Universidad Autónoma de Aguascalientes, Av. Universidad 940, Aguascalientes, México*

Received 30 September 2013; Accepted 20 January 2014

ABSTRACT

This paper reports new insights on the role of the inorganic composition of Bone char (BC) on its sorption properties for the removal of heavy metals Cd^{2+}, Ni^{2+}, and Zn^{2+} ions from aqueous solution. In particular, we showed the importance of both composition and surface chemistry of BC on its sorption properties for the removal of these metal ions in aqueous solution. Results of physicochemical characterization and sorption studies suggest that the inorganic phase of BC may contribute from 60 to 92% of the sorption process of heavy metals in aqueous solution. In particular, the ion exchange process of Ca^{2+} involving the hydroxyapatite has an important contribution in heavy metal removal using bone char. BC is an outstanding sorbent for the removal of Ni^{2+} ions and appears to be suitable for water purification systems.

Keywords: Bone char; Heavy metals; Water treatment; Sorption; Surface chemistry

1. Introduction

Bone char (BC) is a sorbent with outstanding properties for its application in the treatment of wastewaters and industrial effluents polluted by both organic and inorganic compounds [1]. This low-cost sorbent is synthesized from the residues of the meat industry, which generates annually around 500,000 tons of this precursor worldwide. The synthesis of BC implies the pyrolysis or partial calcination of bone wastes using temperatures between 500 and 1,000˚C under controlled atmosphere conditions [2]. Traditionally, BC has been used in sugar industry and is considered among the best sorbents for fluoride removal from water [1,3]. However, other studies have shown that BC can be effective for the removal of dyes, organic matter, radioisotopes, and metal ions in water purification and wastewater treatment, e.g. [4–14].

In particular, BC has been introduced as an alternative and promising sorbent for facing the environmental pollution caused by toxic heavy metals. To date, sorption studies of heavy metals using BC have focused on mono-metallic and multi-metallic systems at batch and dynamic conditions especially using packed-bed sorption columns [4,5,7,15]. Sorption studies on BC for heavy metal removal has mainly focused on the following metallic species: Cr^{6+}, Cd^{2+}, Cu^{2+}, and Pb^{2+}. However, it is convenient to remark that a limited number of authors have studied the details and characteristics of sorption mechanisms involved in the removal of metallic species using BC [1,2,14]. Overall, the available studies have concluded that the metal sorption process using BC appears to be related to three removal mechanisms: ion exchange,

---

*Corresponding author.

dissolution–precipitation reactions, and complexation [9]. These mechanisms are associated to the presence of hydroxyapatite in the BC structure, which plays an important role in the sorption of heavy metals and also allows the ion exchange between calcium and metal ions [2]. But, to the best of our knowledge, there are no studies that quantify and establish the relative importance of BC composition and surface chemistry on heavy metal removal from aqueous solution. This knowledge is fundamental to understand relevant aspects of the sorption process of these priority water pollutants using BC and is also useful to improve the synthesis conditions of BC for maximizing its performance (i.e. sorption capacities) in water purification systems.

Therefore, this study determines the importance of both the composition and surface chemistry of BC on its sorption properties for the removal of heavy metal ions in aqueous solution. Specifically, we have studied the sorption process of Cd^{2+}, Ni^{2+}, and Zn^{2+} ions using BC with and without an acid treatment. This chemical treatment has been employed to modify the BC chemical structure and to determine the role and contribution of inorganic phase of BC on the sorption process of heavy metals. In summary, results of physicochemical characterization and sorption studies suggest that the inorganic phase of BC may contribute up to 92% of the sorption process of heavy metals in aqueous solution.

2. Materials and methods

2.1. Sorbent description and physicochemical characterization

A commercial BC supplied by BC—Carvão Ativado do Brazil Ltda. company has been used in this study. According to the manufacturer, this sorbent is obtained by carbonization of bovine bones at 800˚C under controlled oxygen atmosphere. General sorbent characteristics provided by the supplier are given in Table 1.

Table 1
Properties of commercial BC provided by the supplier

Acid soluble ash (wt.%)	<3
Calcium carbonate (wt.%)	7–9
Calcium sulfate (wt.%)	0.1–0.2
Carbon content (wt.%)	9–11
Hydroxyapatite (wt.%)	70–76
Iron as Fe_2O_3 (wt.%)	<0.3
Density (g/cm^3)	0.65

This BC was washed using boiled deionized water and raw BC (which has been labeled as R-BC) without any further treatment were used in our study. On the other hand, to determine the impact of the inorganic skeleton of BC on its sorption properties, samples of this sorbent were treated with 1 N HNO_3 for 48 h. This acid treatment was used to dissolve the inorganic fraction from BC chemical structure. Results of preliminary studies were used to determine the operating conditions of acid treatment (i.e. the acid concentration and the contact time) to maximize the reduction of this inorganic phase of BC. Sorbent samples obtained from acid treatment have been labeled as AC–BC. Both R–BC and AC–BC samples were finally washed with deionized water at room temperature and dried at 110˚C for 5 h. These samples were grounded and sieved to obtain a mean particle size of 0.3–0.42 mm. This particle size was used in all the experiments performed in the present study.

Physicochemical parameters, textural properties, and composition of the sorbents (i.e. R–BC and AC–BC) were determined using different analytical techniques and results were used to analyze the structural changes caused by the partial removal of the inorganic skeleton of BC. First, the carbon, hydrogen, nitrogen, oxygen, and sulfur contents in the sorbents were determined using appropriate elemental microanalyzers from LECO. Micrographs of sorbents were taken using a Zeiss DSM 942 SEM equipment, in order to observe the morphology of BC before and after the acid treatment. Additionally, the elemental analysis of the sorbent samples was performed by energy dispersive X-ray spectroscopy (EDX) with an Oxford Link ISIS system coupled to SEM. The morphology and chemical composition were determined at different points of each sample and an average of the composition was obtained.

The point of zero charge (pH_{pzc}) of both sorbents was determined at batch conditions. Specifically, samples were placed in contact with NaCl solutions (0.01, 0.1, and 1.0 M) at different pH levels (i.e. from 2 to 9) using a sorbent–electrolyte ratio of 4 g/L. Sorbent and electrolyte solutions were in contact for 72 h at 30˚C in a thermal bath without shaking. After reaching the equilibrium, the pH of the solution was measured. The difference between the initial and final pH of the solutions (i.e. ΔpH) was calculated, and this value was plotted vs. initial pH. The intersection point is where $\Delta pH = 0$ provides the value of pH_{pzc} [16]. Acidity and basicity constants of R–BC and AC–BC were determined by inverse gas chromatography using the Donnet method [17]. This analysis was performed with a gas chromatograph (Perkin Elmer, Auto system XL) equipped with both flame ionization detector and thermal conductivity. Samples were heated for 3 h at

150°C with a heating rate of 5°C/min using He as carrier gas with a flow rate of 30 mL/min. The temperature range for measurements was 100–130°C for R–BC and 130–150°C for AC–BC, respectively. It is important to remark that the samples were analyzed at these temperatures in order to prevent both large and short retention times of the sorbates. Additionally, pH of the BC samples was determined using 4 g of the sorbent in 100 mL of CO_2-free deionized water at 90°C for 15 min [18]. The sorbent was separated from the solution by filtration and the pH was measured at room temperature (i.e. 25°C).

The ash content in both sorbents was determined using the UNE 32004 standard method. For this quantification, 2 g of each sample was heated in a muffle furnace at 815°C for 2 h using air as atmosphere. The ashes were analyzed by X-ray diffraction (XRD). The diffraction patterns were obtained using a Bruker D8 Advanced diffractometer using Cu Kα radiation at 40 kV and 40 mA, over the 2θ range with a step of 0.02° and a scan rate of 5 s. A single Göbel mirror configuration was used to focus and monochromatize the X-rays in the sample, attaining highly efficient parallel beam geometry. Surface functional groups of R–BC and AC–BC were also analyzed by FTIR spectroscopy using a Perkin–Elmer 100 FTIR spectrometer and KBr pellets. These analyzes were recorded in the 4,000–400 cm^{-1} spectral range, with a resolution of 4 cm^{-1}. Sixteen spectral scans were performed on each sample and the average value was used to generate each FTIR spectrum. Finally, the textural properties of the sorbents were determined by N_2 adsorption–desorption isotherms at 77.35 K using an ASAP 2010 Micromeritics equipment. The surface area was calculated by the BET model, while the pore size was obtained according to BJH and *t*-plot method, respectively.

2.2. Determination of sorption properties of BC with and without acid treatment

For studying the importance of the inorganic composition of BC in the removal of Cd^{2+}, Ni^{2+}, and Zn^{2+} ions in aqueous solution, sorption experiments were performed at batch conditions using a sorbent–solution ratio of 0.3 and 2.0 g/L for R–BC and AC–BC, respectively. Stock solutions with an initial concentration of 1,000 mg/L were prepared for the different metal ions by dissolving nitrate salts in deionized water. These solutions were diluted to obtain the metal solutions used for sorption experiments. Sorption kinetics were performed at 200 rpm, 30°C, and pH 5 using an initial metal concentration of 100 mg/L; the sorbent and metal solutions were mixed and interacted by different time intervals (0.5–24 h). These experimental data were used for the calculation of sorption kinetic rates using both the pseudo-first-order and pseudo-second-order models. Additionally, we have performed an analysis of intraparticle diffusion to identify the rate-limiting step in the sorption process of heavy metals using both R–BC and AC–BC. On the other hand, sorption isotherms for each metal ion were obtained using solutions with initial concentrations from 20 to 500 mg/L at 30°C and pH 5. Results obtained from the sorption isotherms of R–BC and AC–BC, respectively, were compared in order to analyze the role of the inorganic skeleton of BC onto the uptake of heavy metals. Langmuir, Freundlich and Sips isotherm equations were used to model the equilibrium sorption data. All kinetic and isotherms expressions used in this study are given in Table 2. Parameters of sorption kinetic and isotherm models were obtained by a non-linear regression using the simulated annealing stochastic method [19]. The fitting goodness of all models was tested by the regression coefficient of determination (R^2), the objective function value (F_{obj}), and the mean absolute percentage deviation. Finally, it should be pointed out that all sorption experiments were performed at a pH below the point of hydrolysis and precipitation (as hydroxides) of metal ions tested. Under these operating conditions, the three metals are present in ionic form.

All sorption experiments were carried out in triplicate and, overall, the percentage difference between replicates was less than 5%. The average of these replicates was used for data analysis. The concentrations of Cd^{2+}, Ni^{2+}, and Zn^{2+} ions in sorption experiments were determined using an atomic absorption spectrophotometer Perkin–Elmer AAnalyst 100 equipped with an air-acetylene burner. The sorption capacity q (mmol/g) was calculated using the mass-balance Eq. (1):

$$q = \frac{(C_0 - C_t)V}{m} \tag{1}$$

where m is the sorbent amount used in the metal sorption experiments in g, V is the volume of the metal solution reported in L, and C_0 and C_t are the initial and the remaining metal concentrations at time t given both in mmol/L, respectively.

3. Results and discussion

3.1. Physicochemical characterization of BC with and without an acid treatment

Results of physicochemical characterization (i.e. pH, acidity/basicity constants, ash content, point of

Table 2
Description of kinetic and isotherm equations employed in the modeling of heavy metal removal using bone char

Model	Equation	Parameters
Kinetic[a]		
Pseudo-first-order	$q_t = q_e(1 - e^{-k_1 t})$	k_1 is the rate constant of pseudo-first-order model in h^{-1} [37].
Pseudo-second-order	$t = \frac{q_e^2 k_2 t}{1+q_e k_2 t}$	k_2 is the sorption rate constant of pseudo-second-order model in g/mmol h [38].
Intraparticle diffusion	$q_t = k_p t^{1/2} + C$	k_p is the intraparticle diffusion rate constant (mmol/g $h^{0.5}$), and C is the constant (mmol/g) used to identify the rate limiting step of the sorption process [39].
Isotherm[b]		
Langmuir	$q_e = \dfrac{q_m K_L C_e}{1 + K_L C_e}$	q_m is a theoretical constant related to sorption capacity (mmol/g) and K_L is the Langmuir constant related to the sorption energy (L/mmol) [40].
Freundlich	$q_e = K_f C_e^{1/n_1}$	K_f (L/g) and n_1 are the Freundlich parameters indicative of sorption capacity and intensity, respectively [41].
Sips	$q_e = \dfrac{a_s b_s C_e^{ns}}{1 + b_s C_e^{ns}}$	a_s is the monolayer of the sorption capacity (mmol/g), b_s is the Sips constant related to the sorption energy, and n_s indicates the sorption intensity [42].

[a] In all kinetic models, q_t is the metal uptake (mmol/g) at time t (h) and q_e is the theoretical sorption capacity (mmol/g) at equilibrium.
[b] In these isotherm models, C_e is the equilibrium concentration (mmol/L) and q_e is the sorption capacity at equilibrium (mmol/g).

zero charge, and textural parameters) of R–BC and AC–BC are reported in Table 3. By comparing the R–BC and AC–BC samples, it is evident that the ash content decreases significantly after acid treatment. This drastic decrement on the ash content indicates that a significant proportion of the inorganic matter of BC was removed by HNO_3. Note that the ash content mainly includes minerals, such as aluminum, iron, silica, calcium, and magnesium [20]. With illustrative purposes, Fig. 1 shows the kinetics of weight loss of BC for different concentrations of HNO_3 used to dissolve the inorganic phase of BC. It is clear that a 1 N acid solution is suitable for dissolving a significant amount of this inorganic phase from BC.

Overall, the acid treatment generates a sorbent with an acidic character while R–BC showed a slightly basic pH. Results of pH_{pzc} are 7.5 and 4.0 for R–BC and AC–BC, respectively. Note that HNO_3 is an oxidant agent and may introduce additional acidic groups on the carbon phase of BC [21]. Table 3 shows the acidic and basic constants of BC before and after being treated with the HNO_3 solution. These results confirmed previous findings and the K_B/K_A ratio indicates the basic ($K_B/K_A > 1$) and acidic ($K_B/K_A < 1$) character of R–BC and AC–BC, respectively. The acidic nature of AC–BC sample could be attributed to the elimination of inorganic compounds originating sites on the carbon fraction of BC, which may chemisorb atmospheric oxygen at room temperature, resulting in the formation of acid complexes on the sorbent surface [21]. These results are consistent with the elemental analysis since the acid treatment increased the oxygen content in the BC from 19.3 to 23.9%. This analysis also indicates that the nitrogen and hydrogen content also increased with this chemical treatment. In summary, the results reported in Table 3 show that a significant proportion of the inorganic components of BC were solubilized with HNO_3 treatment.

Table 3
Results of physicochemical characterization of raw BC (R–BC) and acid-treated BC(AC–BC)

Parameters	Value	
	R–BC	AC–BC
pH	8.28	3.52
pH_{pzc}	7.50	4.00
Ash (%)	81.90	2.03
Acidity/basicity constants		
K_B/K_A	2.37	0.96
Textural properties		
Surface area BET (m^2/g)	113.3	810.9
Micro-pore volume (cm^3/g)	1×10^{-3}	0.07
Micro-pore area (m^2/g)	6.4	145.3
External surface area (m^2/g)	106.8	664.7
Punctual surface area (m^2/g)	110.3	795.6
Total volume (cm^3/g)	0.29	0.64
Pore diameter (Å)	32.5 and 100.8	31.8
Elemental analysis (wt.%)		
Carbon	11.65	69.99
Hydrogen	1.03	2.71
Nitrogen	1.21	5.59
Sulfur	0.06	0.21
Oxygen	19.30	23.90

The morphology and spectra of elemental analysis of R–BC and AC–BC are reported in Fig. 2. The micro-

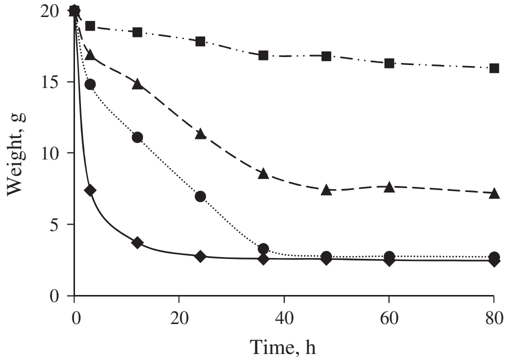

Fig. 1. Kinetics of weight loss of BC treated with HNO_3. Acid concentration: (■) 0.1, (▲) 0.25, (•) 0.5 and (♦) 1 N.

graphs clearly show that the sorbent suffers significant structural changes due to the chemical treatment with HNO_3. In particular, R–BC has an irregular structure and its chemical composition includes the presence of C, O, P, and Ca, which are the main components of hydroxyapatite. On the other hand, the sorbent treated with HNO_3 shows a highly porous structure, which indicates that the acid treatment creates more pores on the sorbent surface and increases the surface area. This porosity increment can be attributed to the dissolution of inorganic components (mainly Ca and P) present in the sorbent. In fact, the micro-analytical spectrum reveals that the C and O are the main components of AC–BC, see Fig. 2(b). These results are consistent with the results of X-ray diffraction (see Fig. 3). In this case, the well-defined XRD peaks of R–BC correspond to the characteristic peaks of calcium phosphate [13]. The most intense peaks appear in 2θ-axis at 20 and 60, which are typical of the apatite phase Fig. 3(a). These results confirmed that R–BC is a mixed sorbent composed of calcium phosphate and amorphous carbon. Note that the calcium phosphate is in the form of hydroxyapatite, while the amorphous carbon fraction is distributed throughout this structure. Similar findings have been reported by Pan et al. [2], Rezaee et al. [11] and Ghanizadeh and Asgari [13]. On the other hand, AC–BC sample is constituted by ferric oxide and silicon dioxide, see Fig. 3(b). These results confirmed again that a significant amount of the inorganic phase was extracted from BC. It is convenient to remark that some trace elements of the bone tissue, e.g. iron and silicon dioxide, were detect on AC–BC samples. In particular, iron ions are among the major trace elements of bone tissue [22], while silicon dioxide is a trace mineral found in bones. The latter is an important component of collagen and is associated with the calcium at an early stage of calcification to keep bones strong [23].

FTIR analysis is given in Fig. 4 where R–BC shows bands of vibrational structure due to the presence of hydroxyl groups and water (3,435 cm^{-1}), nitrogen compounds (2,337 cm^{-1}), and phosphate groups (603 and 1,032 cm^{-1}) on the sorbent surface. The main signal of the phosphate group appears in the triplet located between 1,000 and 1,100 cm^{-1} where these bands are typical of hydroxyapatite [24]. The bands located at 873 cm^{-1} and between 1,500 and 1,350 cm^{-1}, respectively, are attributed to the carbonate group present in the sorbent [24]. After the acid treatment, the FTIR spectrum Fig. 4(b) shows that the intensity of bands of carbonates and phosphates reduced drastically because the HNO_3 dissolved a significant amount of these compounds and, consequently, they are released from the sorbent. Specifically, the most important changes in the FTIR spectrum of AC–BC are observed at 2,400–500 cm^{-1}. Finally, the broad band located at 1,079 cm^{-1} is assigned to vibrations of type Si-O and the peak at 511 cm^{-1} could be assigned to the bending frequency of O–Si–O, which confirms the presence of silicon dioxide in the sample [25,26].

N_2 adsorption–desorption isotherms show that R–BC and AC–BC presented a type IV isotherm according to the BDDT classification, see Fig. 5. There are hysteresis loops of types H_3 and H_2 in the R–BC and AC–BC, respectively, according to the IUPAC classification. Hysteresis loop H_3 is attributed to the presence of mesopores surrounded by a matrix of smaller pores, which is associated to particles agglomerates that have slit-shaped pores [27,28]. On the other hand, the hysteresis loop H_2 is attributed to the presence of relatively uniform pores in the form of channels [28]. Finally, it is evident that N_2 adsorption is greater for AC–BC than R-BC, indicating that the first sorbent has a greater surface area. Textural parameters of both sorbents are also reported in Table 3. In general, R–BC has a distribution of different pore sizes showing two maximum points whose values are 32.5 and 100.0 Å, respectively; while AC–BC shows a mono-modal distribution with an average particle size of 34.5 Å, see Fig. 5(b). Note that the pore size is homogeneous in the sorbent after the acid treatment and there is an increment in the pore volume; see results reported in Table 3.

3.2. Sorption properties of BC with and without acid treatment for the removal of heavy metals

With illustrative purposes, Fig. 6 shows the kinetic data obtained for the sorption of Cd^{2+}, Ni^{2+}, and Zn^{2+} ions in aqueous solution at 30°C, pH 5, and an initial

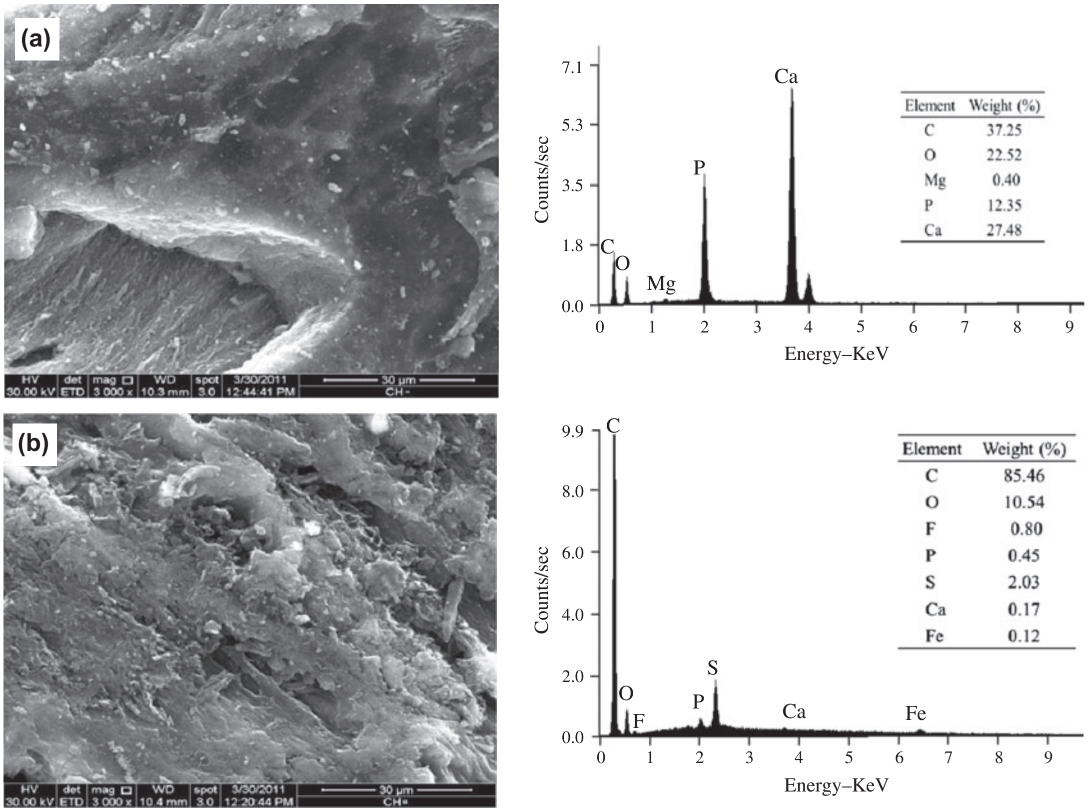

Element	Weight (%)
C	37.25
O	22.52
Mg	0.40
P	12.35
Ca	27.48

Element	Weight (%)
C	85.46
O	10.54
F	0.80
P	0.45
S	2.03
Ca	0.17
Fe	0.12

Fig. 2. Scanning electron micrographs and elemental compositions of (a) R–BC and (b) AC–BC.

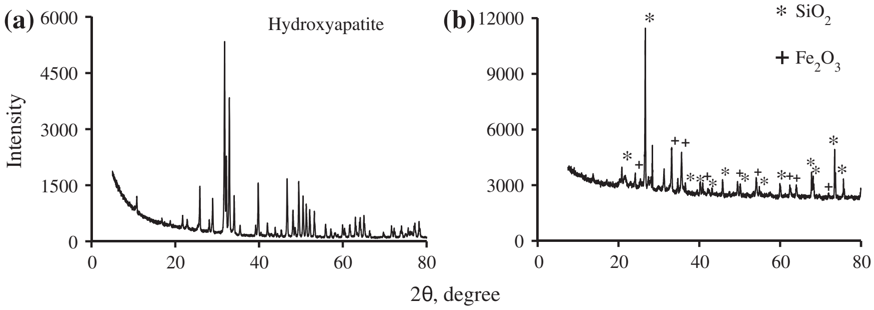

Fig. 3. Results of X-ray diffraction of (a) R–BC and (b) AC–BC.

metal concentration of 100 mg/L for both R–BC and AC–BC. Overall, the removal of metal ions increased with time and was fast during the first 4 h, regardless of the cation. Later, the sorption rate decreased gradually and all the kinetics reached the equilibrium at 12 h. Sorption kinetic profile of both sorbents corresponds to a continuous curve which reaches the saturation and suggests the possible coverage of the sorbent surface with a monolayer of metal ion. Kinetic parameters calculated with the pseudo-first- and pseudo-second-order models are reported in Table 4. Sorption rates (k_1 and k_2) of AC–BC are lower than those obtained with R–BC where the pseudo-first-order model offered the best correlation of kinetic data. Note that the sorption rates of the metal ions decreased in the following order: $Ni^{2+} > Zn^{2+} > Cd^{2+}$. On the other hand, Fig. 7 shows the analysis of intraparticle diffusion for the kinetic data obtained in

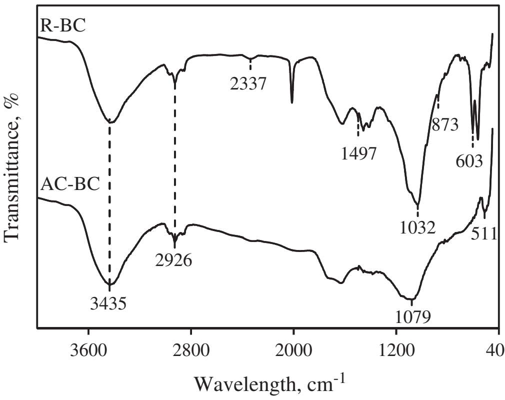

Fig. 4. FTIR spectra of R–BC and AC–BC.

this study. These results indicate that the metal sorption using R–BC and AC–BC can be associated to a fast external surface sorption and intraparticle diffusion [29]. However, the intraparticle diffusion is not the controlling step of metal sorption process of both R–BC and AC–BC. The contribution of surface sorption as the controlling step of heavy metal removal is more significant for R–BC because this sorbent showed higher values of the intercept *C* than those obtained with AC–BC, see Table 4.

Sorption isotherms of Cd^{2+}, Ni^{2+}, and Zn^{2+} at pH 5 and 30°C using R–BC and AC–BC are reported in Fig. 8. All sorption isotherms are regular, positive, and concave with respect to the concentrations axis. These isotherms are class “L” (Langmuir) type 2 according to the Giles classification and indicate that the metal sorption is favorable [30]. Maximum metal uptakes of R–BC are: 0.70 mmol/g for Cd^{2+}, 5.3 mmol/g for Ni^{2+}, and 0.63 mmol/g for Zn^{2+}; while AC–BC showed maximum sorption capacities of 0.18 mmol/g for Cd^{2+}, 0.38 mmol/g for Ni^{2+}, and 0.27 mmol/g for Zn^{2+}, respectively. Metal sorption capacity of AC–BC increases in the following order: $Cd^{2+} < Zn^{2+} < Ni^{2+}$, while R–BC shows the following removal behavior: $Zn^{2+} < Cd^{2+} << Ni^{2+}$. It is evident that sorption capacity of R–BC is higher than that obtained using AC–BC. In fact, the sorption properties of BC treated with HNO_3 decreased in 74, 92, and 57% for the removal of Cd^{+2}, Ni^{+2} and Zn^{+2}, respectively. Similar results have been reported by Dahbi et al. [31] for the removal of

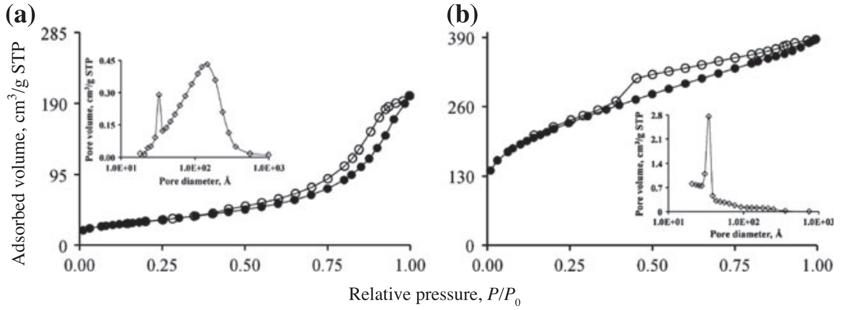

Fig. 5. N_2 adsorption–desorption isotherms (at 77.35 K) and pore size distribution of (a) R–BC and (b) AC–BC. (•) Adsorption and (○) Desorption.

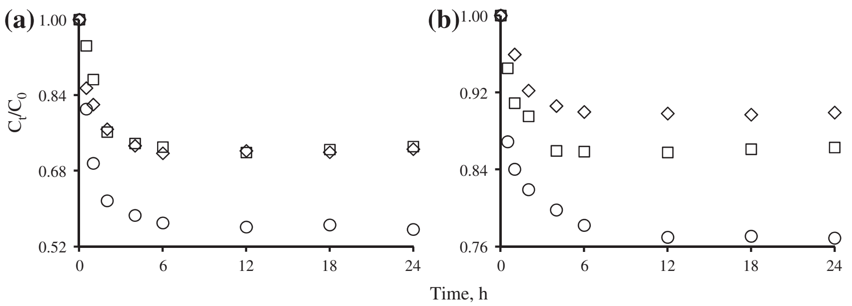

Fig. 6. Sorption kinetics of (□) Cd^{2+}, (○) Ni^{2+}, and (◊) Zn^{2+} using (a) R–BC and (b) AC–BC. Experimental conditions: sorbent ratio of 0.3 g/L and 4 g/L for R–BC and AC–BC, respectively, 30°C, pH 5, and initial metal concentration of 100 mg/L.

Table 4
Results of kinetic data modeling of the sorption of Cd^{2+}, Ni^{2+}, and Zn^{2+} using R–BC and AC–BC

Sorbent	Model	Cd^{2+}	Ni^{2+}	Zn^{2+}
R-BC	Pseudo-first-order			
	k_1, h^{-1}	0.35	1.10	0.48
	q_1, mmol/g	0.98	1.63	0.55
	R^2	0.96	0.81	0.97
	F_{obj}	0.02	0.05	0.02
	E_{abs}	3.87 ± 4.13	7.43 ± 3.32	3.83 ± 4.27
	Pseudo-second-order			
	k_2, g/mmol h	0.39	1.18	0.54
	q_2, mmol/g	3.21	2.03	1.20
	R^2	0.94	0.97	0.86
	F_{obj}	0.03	0.01	0.07
	E_{abs}	5.54 ± 3.05	2.86 ± 1.48	8.73 ± 4.93
	Intraparticle diffusion			
	k_p, mmol/g $h^{0.5}$	0.10	0.18	0.10
	C, mmol/g	0.13	0.67	0.22
	R^2	0.82	0.99	0.97
	F_{obj}	0.01	3×10^{-7}	9×10^{-4}
	E_{abs}	4.77 ± 2.59	0.03 ± 0.01	8.30 ± 8.06
AC–BC	Pseudo-first-order			
	k_1, h^{-1}	0.13	0.37	0.21
	q_1, mmol/g	0.52	1.16	1.29
	R^2	0.90	0.99	0.94
	F_{obj}	0.10	3×10^{-3}	0.03
	E_{abs}	8.09 ± 8.03	1.64 ± 1.08	5.05 ± 3.91
	Pseudo-second-order			
	k_2, g/mmol h	0.15	0.40	0.22
	q_2, mmol/g	3.54	3.77	8.38
	R^2	0.81	0.96	0.97
	F_{obj}	0.20	0.02	0.01
	E_{abs}	13.57 ± 8.94	4.35 ± 2.56	2.94 ± 2.09
	Intraparticle diffusion			
	k_p, mmol/g $h^{0.5}$	0.01	0.04	0.04
	C, mmol/g	0.09	0.27	0.12
	R^2	0.95	0.99	0.98
	F_{obj}	3×10^{-4}	7×10^{-5}	3×10^{-4}
	E_{abs}	1.04 ± 0.49	0.47 ± 0.22	1.03 ± 0.50

Cr^{3+} ions in wastewater using BC. These authors used BC treated with HNO_3 and concluded that the sorption capacity of this treated sorbent reduced drastically in comparison to the results obtained with raw BC. As stated, the basic character of R–BC favors the removal of metal ions since they have a positive charge and, consequently, the interactions between this sorbent and the pollutants are favored. Results of isotherm data modeling are reported in Table 5. Sips equation showed the best performance for modeling the equilibrium sorption data for the different heavy metals and both sorbents and parameters of this model are given in Table 6. Finally, Langmuir model is better than Freundlich isotherm for fitting the experimental data obtained in this study.

In summary, sorption results suggest that the inorganic skeleton of BC play an important role in the removal of metal ions. According to the available literature [2], the inorganic fraction of BC is useful for the sorption of cations and also allows an ion exchange process between the metal species and Ca^{2+} ions. Based on this fact, the Ca^{2+} content in the solutions before and after the removal process was quantified for sorption experiments using atomic absorption spectroscopy. Results of these quantifications were used to calculate the molar ratios (Q_+) of metals fixed

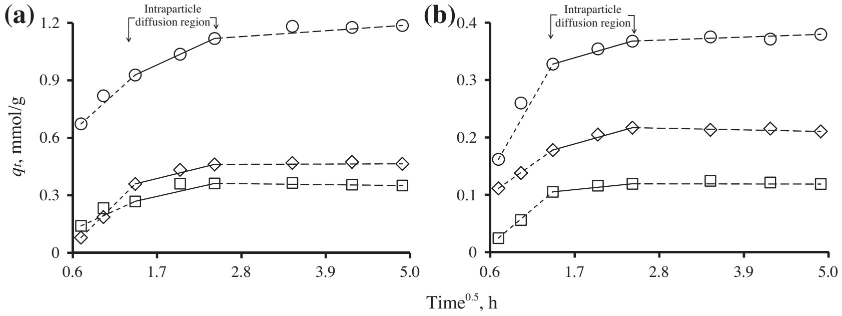

Fig. 7. Intraparticle diffusion analysis for the sorption of (□) Cd^{2+}, (○) Ni^{2+}, and (◇) Zn^{2+} using a) R–BC and b) AC–BC. Operating conditions: 30°C, pH 5, and initial metal concentration.

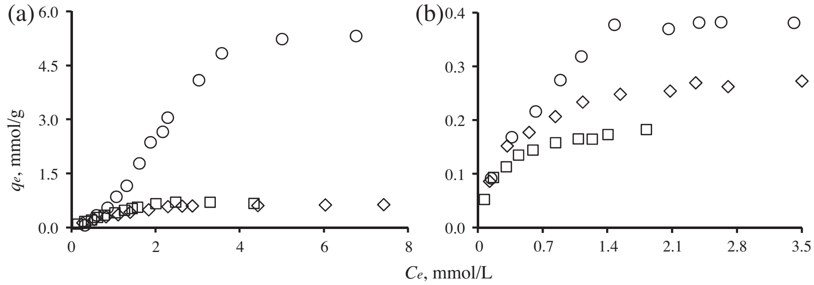

Fig. 8. Sorption isotherms of (□) Cd^{2+}, (○) Ni^{2+}, and (◇) Zn^{2+} using (a) R–BC and (b) AC–BC at 30°C and pH 5.

by both R–BC and AC–BC to Ca^{2+} ion released. Note that $Q_+ = 1$ indicates the possible presence of ion exchange, while $Q_+ > 1$ suggests a surface complexation as the main sorption mechanism [32]. Therefore, the calculated ratios were used to estimate the possible contribution of the ion exchange process in the removal of these metal ions. Fig. 9 shows the results obtained for Ca^{2+} determinations in sorption experiments. For R-BC, Q_+ ranged from 0.4 to 1.3, while $Q_+ > 4$ for AC–BC. It appears that the ion exchange may be involved in the heavy metal removal using R-BC, while the metal uptake using AC–BC seems to be associated to surface complexation. Note that the content of Ca^{2+} released when Ni^{2+} ions were removed is higher than the quantities obtained during the removal of Zn^{2+} and Cd^{2+} ions, see Fig. 9. This information is consistent with the results of the sorption isotherms where both sorbents showed the maximum uptake for this metal ion. On the other hand, results of kinetic experiments suggest that the removal rate of heavy metals is directly proportional to the released amount of Ca^{2+} ions. This trend suggests that the ion exchange appears to have a relevant contribution for the mass transfer mechanisms involved in heavy metal removal especially for R-BC. Therefore, the removal of these pollutants appears to be faster when there is a high content of Ca^{2+} on the sorbent, since the number of available ion exchange sites is greater. Finally, it is convenient to remark that the extent of ion exchange process is related to the properties of interchangeable cations. Previous studies have concluded that cations with an ionic radius smaller than Ca^{2+} (1.74 Å) can be exchanged more easily [33]. Our sorption results are in accordance with this fact where the metal uptakes has the following order: Ni^{2+} (1.21 Å) > Zn^{2+} (1.31 Å) > Cd^{2+} (1.48 Å).

Table 5
Results of data modeling of sorption isotherms of Cd^{2+}, Ni^{2+}, and Zn^{2+} on R–BC and AC–BC

		Statistical analysis		
Sorbent	*Model*	*R^2*	*E, %*	*F_{obj}*
R-BC	Freundlich	0.52–0.93	7.05–36.09	0.09–1.97
	Langmuir	0.15–0.98	5.14–67.67	0.05–16.90
	Sips	0.97–0.99	4.73–6.01	0.04–0.09
AC–BC	Freundlich	0.90–0.93	7.50–9.31	0.06–0.13
	Langmuir	0.97–0.99	1.79–4.53	0.01–0.03
	Sips	0.97–0.99	1.59–4.20	4×10^{-3}–0.03

Table 6
Parameters of the Sips model obtained from data fitting of sorption isotherms of Cd^{2+}, Ni^{2+} and Zn^{2+} using R–BC and AC–BC

Sorbent	Metal	q_s, mmol/g	b_s, L/mmol	n_s	R^2	F_{obj}	E_{abs}
A-BC	Ni^{2+}	6.22	0.42	2.24	0.99	0.09	6.01 ± 6.02
	Zn^{2+}	0.75	0.92	1.14	0.97	0.04	4.93 ± 2.63
	Cd^{2+}	1.51	0.33	0.90	0.98	0.04	4.72 ± 3.98
AC–BC	Ni^{2+}	0.50	1.37	0.93	0.97	0.03	4.19 ± 3.84
	Zn^{2+}	0.31	2.7	0.90	0.99	0.01	2.14 ± 1.25
	Cd^{2+}	0.20	4.71	0.90	0.99	4×10^{-3}	1.58 ± 1.26

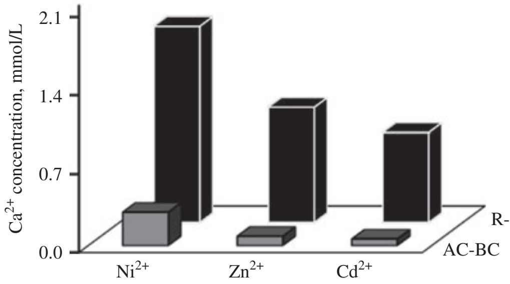

Fig. 9. Content of calcium released in sorption experiments of Cd^{2+}, Ni^{2+}, and Zn^{2+} using R–BC and AC–BC.

3.3. *Removal mechanism of heavy metals using BC with and without acid treatment*

Results of sorption experiments and sorbent characterization indicate that the removal of heavy metals may involve ion exchange and complex formation on the sorbent surface as the main removal mechanisms depending on if R–BC or AC–BC is used. For the case of R-BC, the sorption of heavy metal could be attributed to the following mechanisms [1,32] given by Eqs. (2) and (3):

$$\equiv Ca^{2+} + M^{2+} = \equiv M^{2+} + Ca^{2+} \tag{2}$$

$$\equiv OH + M^{2+} = \equiv O - M^{+} + H^{+} \tag{3}$$

where M^{2+} is the metal ion in aqueous solution and ≡ symbolizes the sorbent surface, respectively. Note that Eq. (3) is used for representing the interactions with heavy metals and calcium phosphate of BC [1]. On the other hand, the silicon and iron compounds of the AC–BC appear to have an important role in the removal of heavy metals through complexation reactions [34]. Therefore, the sorption mechanism for Cd^{2+}, Ni^{2+}, and Zn^{2+} when AC–BC is used as sorbent

Table 7
Survey of sorption capacities reported for the removal of heavy metal using different sorbents

Metal	Sorbent	q_e[a] (mmol/g)	pH	T (℃)	Reference
Cd^{2+}	Hydroxyapatite	0.58	NS	26	[33]
	Bone char	0.48	5.0	20	[15]
	Hydroxyapatite	1.68	NS	25	[32]
	Modified rice husk	0.18	NS	NS	[43]
	Modified orange peel	0.64	7.0	25	[36]
Ni^{2+}	Coir pith	1.06	NS	NS	[43]
	Groundnut shells	0.13	NS	NS	[43]
	Modified sawdust	0.18	NS	NS	[43]
	Bone char	0.55	5.1	25	[14]
Zn^{2+}	Hydroxyapatite	0.57	NS	26	[33]
	Bone char	0.53	4.8	20	[44]
	Bone char	0.51	5.0	20	[15]
	Modified sawdust	0.24	NS	NS	[43]
	Carrot residues	0.45	NS	NS	[43]

[a] Maximum sorption capacity. NS indicates that the pH or temperature is not specified in the reference.

could be a combination of ion exchange and complexation reactions. According to [35,36], these reactions can be represented by Eqs. (4) and (5):

$$\equiv\text{FeOH} + \text{M}^{2+} = \equiv\text{FeO} - \text{M}^{+} + \text{H}^{+} \quad (4)$$

$$\equiv\text{SiOH} + \text{M}^{2+} = \equiv\text{SiO} - \text{M}^{+} + \text{H}^{+} \quad (5)$$

However, it is important to note that the ion exchange involving Ca^{2+} appears to have a limited contribution on the removal mechanism when AC–BC is used because the amount of Ca^{2+} released is very low. This fact is consistent with the calcium content in the HNO_3-treated sorbent, since this element represents only a 0.17% of the sample. In summary, we can conclude that the inorganic fraction of BC has an important role for the removal of metal ions from aqueous solution.

Finally, for comparison purposes, Table 7 shows some sorption capacities reported in literature for the removal of Cd^{2+}, Ni^{2+}, and Zn^{2+} in aqueous solution using different sorbents. In general, we conclude that BC is an interesting sorbent for the treatment of effluents polluted with these heavy metals. In particular, this sorbent is attractive for the removal of Ni^{2+} since it can show a sorption capacity up to 15% of its weight, which is an outstanding performance based on the fact that most of the commercial sorbents showed lower metal uptakes.

4. Conclusions

Sorption properties of BC for the removal of heavy metal ions are highly dependent on the inorganic composition fraction of this sorbent. In particular, calcium phosphate is the main inorganic component of BC and appears to be responsible for more than 60% of the removal process of heavy metals. The ion exchange process of Ca^{2+} involving the hydroxyapatite has an important contribution in heavy metal removal using bone char. Sorption results also indicated that the affinity of BC for the different cations depends on the physicochemical properties of the solute where the ionic radius seems to be the dominant factor. BC is an outstanding sorbent for the removal of Ni^{2+} ions and appears to be suitable for water purification systems.

References

[1] S.S.M. Hassan, N.S. Awwad, A.H.A. Aboterika, Removal of mercury(II) from wastewater using camel bone charcoal, J. Hazard. Mater. 154 (2008) 992–997.

[2] X. Pan, J. Wang, D. Zhang, Sorption of cobalt to bone char: Kinetics, competitive sorption and mechanism, Desalination 249 (2009) 609–614.

[3] N.A. Medellin-Castillo, R. Leyva-Ramos, R. Ocampo-Perez, R.F. Garcia de la Cruz, A. Aragon-Piña, J.M. Martinez-Rosales, R.M. Guerrero-Coronado, L. Fuentes-Rubio, Adsorption of fluoride from water solution on bone char, Ind. Eng. Chem. Res. 46 (2007) 9205–9212.

[4] D.C.K. Ko, J.F. Porter, G. McKay, Optimised correlations for the fixed-bed adsorption of metal ions on bone char, Chem. Eng. Sci. 55 (2000) 5819–5829.

[5] C.W. Cheung, D.C.K. Ko, J.F. Porter, G. McKay, Binary metal sorption on BC mass transport model using IAST, Langmuir 19 (2003) 4144–4153.

[6] K.K.H. Choy, D.C.K. Ko, C.W. Cheung, J.F. Porter, G. McKay, Film and intraparticle mass transfer during the adsorption of metal ions onto bone char, J. Colloid. Interf. Sci. 271 (2004) 284–295.

[7] D.C.K. Ko, C.W. Cheung, K.K.H. Choy, J.F. Porter, G. McKay, Sorption equilibria of metal ions on bone char, Chemosphere 54 (2004) 273–281.

[8] C.W. Cheung, K.K.H. Choy, J.F. Porter, G. Mckay, Empirical multicomponent equilibrium and film-pore model for the sorption of copper, cadmium and zinc onto bone char, Adsorption 11 (2005) 15–29.

[9] K. Chojnacka, Equilibrium and kinetic modelling of chromium(III) sorption by animal bones, Chemosphere 59 (2005) 315–320.

[10] Y.N. Chen, L.Y. Chai, Y.D. Shu, Study of arsenic(V) adsorption on BC from aqueous solution, J. Hazard. Mater. 160 (2008) 168–172.

[11] A. Rezaee, Gh Ghanizadeh, Gh Behzadiyannejad, A. Yazdanbakhsh, S.D. Siyadat, Adsorption of endotoxin from aqueous solution using bone char, B. Environ. Contam. Tox. 82 (2009) 732–737.

[12] B.R. Ferreira, R. Marinuchi, G.J. Martins, O.I. Conceição, A.A. Augusto, T.C.R. Granhen, M.A.S.D. Barros, Equilibrium studies of Mn(II), Pb(II) and Cr(III) in bone char, Chem. Eng. Trans. 21 (2010) 721–726.

[13] Gh Ghanizadeh, G. Asgari, Adsorption kinetics and isotherm of methylene blue and its removal from aqueous solution using bone charcoal, React. Kinet. Mech. Cat. 102 (2010) 124–142.

[14] J.C. Moreno, R. Gómez, L. Giraldo, Removal of Mn, Fe, Ni and Cu ions from wastewater using cow bone charcoal, Materials 3 (2010) 452–466.

[15] K.K.H. Choy, G. McKay, Sorption of cadmium, copper, and zinc ions onto BC using Crank diffusion model, Chemosphere 60 (2005) 1141–1150.

[16] A.P. Vieira, S.A.A. Santana, C.W.B. Bezerra, H.A.S. Silva, J.C.P. de Melo, Edson C. da Silva Filho, C. Airoldi, Copper sorption from aqueous solutions and sugar cane spirits by chemically modified babassu coconut (*Orbignya speciosa*) mesocarp, Chem. Eng. J. 161 (2010) 99–105.

[17] J.B. Donnet, S.J. Park, H. Balard, Evaluation of specific interactions of solid surfaces by inverse gas chromatography, Chromatographia 31 (1991) 434–440.

[18] D. Kalderis, S. Bethanis, P. Paraskeva, E. Diamadopoulos, Production of activated carbon from bagasse and rice husk by a single-stage chemical activation method at low retention times, Bioresour. Technol. 99 (2008) 6809–6816.

[19] A. Bonilla-Petriciolet, M.G. Lira-Padilla, C.A. Soto-Becerra, Aplicación del método de optimización de recocido simulado en la regresión de isotermas de adsorción, Rev. Int. Contam. Ambient. 21 (2005) 201–206.

[20] C.P. Dwivedi, J.N. Sahu, C.R. Mohanty, B.R. Mohan, B.C. Meikap, Column performance of granular activated carbon packed bed for Pb(II) removal, J. Hazard. Mater. 156 (2008) 596–603.

[21] S. Wang, Z. Zhu, Effects of acidic treatment of activated carbons on dye adsorption, Dyes Pigm. 75 (2007) 306–314.

[22] M. Unger, B.M.A. Chiappe, Importancia fisiológica de los microminerales en el metabolismo óseo, Redvet. IX (2008)1695–7504.

[23] E.M. Carlisle, Silicon as a trace nutrient, Sci. Total Environ. 73 (1988) 95–106.

[24] H.Y. Xu, L. Yang, P. Wang, Y. Liu, M.S. Peng, Kinetic research on the sorption of aqueous lead by synthetic carbonate hydroxyapatite, J. Environ. Manage. 86 (2008) 319–328.

[25] O. Prieto, M.A. Vicente, M.A. Bañares-Muñoz, Study of the porous solids obtained by acid treatment of a high surface area Saponite, J. Porous Mat. 6 (1999) 335–344.

[26] K. Baltakys, R. Jauberthie, R. Siauciunas, R. Kaminskas, Influence of modification of SiO_2 on the formation of calcium silicate hydrate, Mater. Sci-Poland 25 (2007) 663–670.

[27] G. Leofanti, M. Padovan, G. Tozzola, B. Venturelli, Surface area and pore texture of catalysts, Catal. Today 41 (1998) 207–219.

[28] L. Zhang, X. Wang, M. Millet Jean-Marc, P.H. Matter, U.S. Ozkan, Investigation of highly active Fe–Al–Cu catalysts for water-gas shift reaction, Appl. Catal. A—Gen. 351(2008) 1–8.

[29] V. Vadivelan, K.V. Kumar, Equilibrium, kinetics, mechanism, and process design for the sorption of methylene blue onto rice husk, J. Colloid Interf. Sci. 286 (2005) 90–100.

[30] E. Gonzalez-Serrano, T. Cordero, J. Rodriguez-Mirasol, L. Cotoruelo, J.J. Rodriguez, Removal of water pollutants with activated carbons prepared from H_3PO_4 activation of lignin from kraft black liquors, Water Res. 38 (2004) 3043–3050.

[31] S. Dahbi, M. Azzi, N. Saib, M. de la Guardia, R. Faure, R. Durand, Removal of trivalent chromium from tannery wastewaters using bone charcoal, Anal. Bioanal. Chem. 374 (2002) 540–546.

[32] A. Corami, S. Mignardi, V. Ferrini, Cadmium removal from single-and multi-metal (Cd + Pb + Zn + Cu) solutions by sorption on hydroxyapatite, J. Colloid Interf. Sci. 317 (2008) 402–408.

[33] Y. Xu, F.W. Schwartz, S.J. Traina, Sorption of Zn^{2+} and Cd^{2+} on Hydroxyapatite Surfaces, Environ. Sci. Technol. 28 (1994) 1472–1480.

[34] A. Papandreou, C.J. Stournaras, D. Panias, Adsorption of Cu(II) on ceramic structures made from greek fly ash, Proceedings of the 9th International Conference on Environ. Sci. Technol. (2005) A1181–A1187.

[35] H.B. Bradl, Adsorption of heavy metal ions on soils and soils constituents, J. Colloid Interf. Sci. 277 (2004) 1–18.

[36] V.K. Gupta, A. Nayak, Cadmium removal and recovery from aqueous solutions by novel adsorbents prepared from orange peel and Fe_2O_3 nanoparticles, Chem. Eng. J. 180 (2012) 81–90.

[37] S. Lagergren, Zur theorie der sogenannten adsorption gelöster stoffe, Kungliga Svenska Vetenskapsakademiens, Handlingar 24 (1898) 1–39.

[38] Y.S. Ho, G. McKay, Pseudo-second order model for sorption processes, Process Biochem. 34 (1999) 451–465.

[39] W.J. Weber, J.C. Morris, Kinetics of adsorption on carbon from solution, J. San. Engin. Div. 89 (1963) 31–60.

[40] I. Langmuir, The constitution and fundamental properties of solids and liquids. Part I. Solids, J. Am. Chem. Soc. 38 (1916) 2221–2295.

[41] H. Freundlich, KapillarChemie, Leipzig, (1909) p. 1181

[42] R. Sips, On the structure of a catalyst surface, J. Chem. Phys. 16 (1948) 490–495.

[43] W.S. Wan Ngah, M.A. Hanafiah, Removal of heavy metal ions from wastewater by chemically modified plant wastes as adsorbents: A review, Bioresour. Technol. 99 (2008) 3935–3948.

[44] C.W. Cheung, J.F. Porter, G. McKay, Removal of Cu(II) and Zn(II) ions by sorption onto BC using batch agitation, Langmuir 18 (2002) 650–656.